Supporting Information

Comparative Spectroscopic Studies on Porphyrin Derivatives: Electronic Perturbation of N-confused and N-fused Porphyrins

Jae Seok Lee,[a] Jong Min Lim,[a] Motoki Toganoh [b], Hiroyuki Furuta*[b]
and Dongho Kim*[a]

[a] *Department of Chemistry, Yonsei University, Seoul 120-749, Korea*
[b] *Department of Chemistry and Biochemistry, Graduate School of Engineering, Kyushu University, Fukuoka 819-0395, Japan.*

*To whom it may correspondence should be addressed.
E-mail: dongho@yonsei.ac.kr; hfuruta@cstf.kyushu-u.ac.jp

Experimental Section

Steady-state Absorption and Fluorescence. Steady-state absorption spectra were obtained using an UV-VIS-NIR spectrometer (Varian, Cary5000) and steady-state fluorescence were measured by a Hitachi model F-2500 fluorometer at room temperature. For the observation of steady-state fluorescence spectra in NIR region, a photomultiplier tube (Hamamatsu, R5108 and H9170-75), a lock-in amplifier (EG&G, 5210) combined with a mechanical chopper and a CW He-Cd laser (Melles Griot, Omnichrome 74) for photo-excitation at 442 nm were used.

Time-Resolved Fluorescence Measurements. Time-resolved fluorescence was detected using a time-correlated single-photon counting (TCSPC) technique. A homemade cavity-dumped Ti:sapphire oscillator pumped by a CW Nd:YVO_4 laser (Coherent, Verdi) was used as the excitation light source; this provided ultrashort pulses (100 fs of full width at half-maximum (fwhm)) and allowed for a high repetition rate (200-400 kHz). The output pulses of the oscillator were frequency-doubled with a second harmonic BBO crystal. The TCSPC detection system consisted of a multichannel plate photomultiplier (Hamamatsu, R3809U-51) with a cooler (Hamamatsu, C4878), a TAC (time-to-amplitude converter) (EG&G Ortec, 457), two discriminators (EG&G Ortec, 584 (signal) and Canberra, 2126 (trigger)), and two wideband amplifiers (Philip Scientific (signal) and a Mini Circuit (trigger)). A personal computer with a multichannel analyzer (Canberra, PCA3) was used for data storage and processing. The decay fittings were made by using a least-squares deconvolution fitting process (LIFETIME program with an iterative nonlinear least-squares deconvolution procedure developed at the University of Pennsylvania). Quartz cell with optical path length of 10 mm was used for all steady-state experiments and time-resolved fluorescence measurements.

Femtosecond Transient Absorption Measurements. The femtosecond time-resolved transient absorption (TA) spectrometer consisted of a homemade noncollinear optical parametric amplifier (NOPA) pumped by a Ti:sapphire regenerative amplifier system (Quantronix, Integra-C) operating at 1 kHz repetition rate and an optical detection system. The generated visible NOPA pulses had a pulse width of ~ 100 fs and an average power of 1 mW in the range 500-700 nm which were used as pump pulses. White light continuum (WLC) probe pulses were generated using a sapphire window (2 mm of thickness) by focusing of small portion of the fundamental 800 nm pulses which was picked off by a quartz plate before entering to the NOPA. The time delay between pump and probe beams was carefully controlled by making the pump beam travel along a variable optical delay (Newport, ILS250). Intensities of the spectrally dispersed WLC probe pulses are monitored by miniature spectrograph (OceanOptics, USB2000+). To obtain the time-resolved transient absorption difference signal (ΔA) at a specific time, the pump pulses were chopped at 25 Hz and absorption spectra intensities were saved alternately with or without pump pulse. Typically, 6000 pulses excite samples to obtain the TA spectra at a particular delay time. The polarization angle between pump and probe beam was set at the magic angle (54.7°) in order to prevent polarization-dependent signals. Cross-correlation fwhm in pump-probe experiments was less than 200 fs and chirp of WLC probe pulses was measured to be 800 fs in the 400-800 nm region. To minimize chirp, all reflection optics in probe beam path and 2 mm path length of quartz cell were used.

Two-photon Absorption Cross-Section ($\sigma^{(2)}$). The TPA measurements were performed using the open-aperture Z-scan method with 130 fs pulses from an optical parametric amplifier (Light Conversion, TOPAS) operating at a 2 kHz repetition rate using a Ti:sapphire regenerative amplifier system (Spectra-Physics, Hurricane X). After passing through a f = 10 cm lens, the laser beam was focused to 1 mm-quartz cell. As the position of the sample cell was varied along the laser-beam direction (z-axis), the transmitted laser beam from the sample cell was then probed using a Ge/PN photodiode (New Focus, 2033) as used for reference monitoring. Assuming a Gaussian beam profile, the nonlinear absorption coefficient β can be obtained by curve fitting to the observed open aperture traces with the following equation:[S1]

$$T(z) = 1 - \frac{\beta I_0 (1 - e^{-\alpha_0 l})}{2\alpha_0 (1 + (z/z_0)^2)},$$

where α_0 is a linear absorption coefficient, I_0 is the on-axis peak intensity of the incident pulses at the focal point, l is a sample length, and z_0 is the diffraction length of the incident beam. After obtaining the nonlinear absorption coefficient β, the TPA cross-section $\sigma^{(2)}$ (in unit of 1 GM = 10^{-50} cm^4 ·s·photon^{-1}molecule^{-1}) of a single solute molecule can be determined by using the following relationship:

$$\beta = \frac{\sigma^{(2)} N_A d \times 10^{-3}}{hv}$$

where N_A is the Avogadro constant, d is the concentration of the TPA compound in solution, h is Planck's constant, and v is the frequency of the incident laser beam. The TPA cross-section value of AF-50 was measured as a reference compound, which was found to exhibit a TPA value of 50 GM at 800 nm.[S2]

Computational Method. Quantum mechanical calculation were performed with the Gaussian 03 program suite.[S3] All calculations were carried out by the density functional theory (DFT) method with Becke's three-parameter hybrid exchange functionals and the Lee-Yang-Parr correlation functional (B3LYP),[S4,S5] employing the 6-31G* basis set. The X-ray crystal structures of **TPP, NCP, NFP, N$_2$FP** were used as initial geometry for geometry optimization without any modification and were used for time dependent density functional theory (TDDFT). The AICD plots were obtained with the Continuous Set of Gauge Transformations (CSGT) method[S6,S7,S8] at the B3LYP/6-311G** level based on the geometry optimized structure modified by replacing *meso*-substituents with hydrogens. The molecular orbitals and AICD results were visualized using Gauss View.[S9]

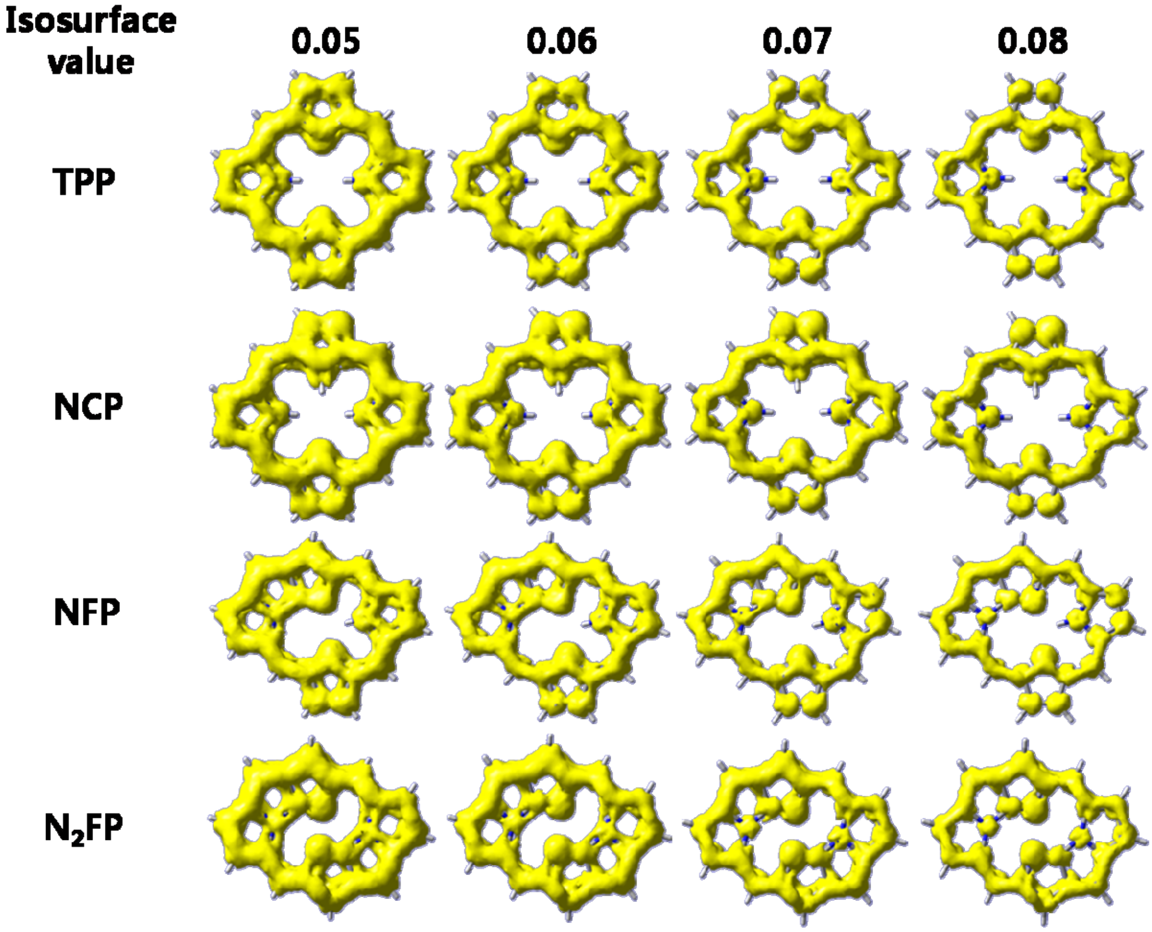

Fig. S1 AICD plots of **TPP**, **NCP**, **NFP**, and **N$_2$FP** upon increasing isosurface values of 0.05 to 0.08.

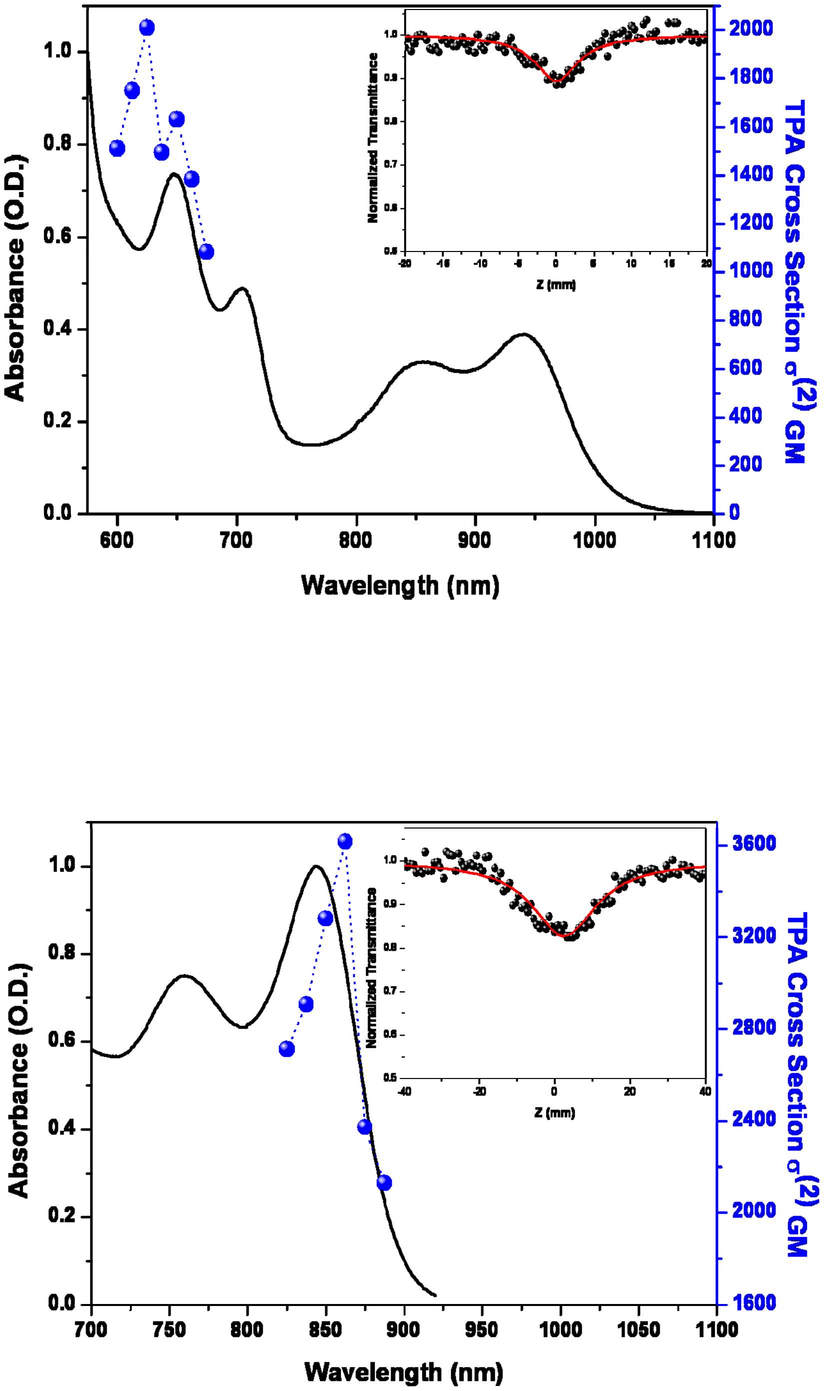

Fig. S2 Two-photon absorption spectra (blue) and Z-scan trace at 1250 and 1725 nm (inset) of **NFP** (top) and **N$_2$FP** (bottom) in CH_2Cl_2, respectively. The solid line indicates the steady-state absorption spectrum for comparison, and the solid line in inset is the best curve fit line of experimental data.

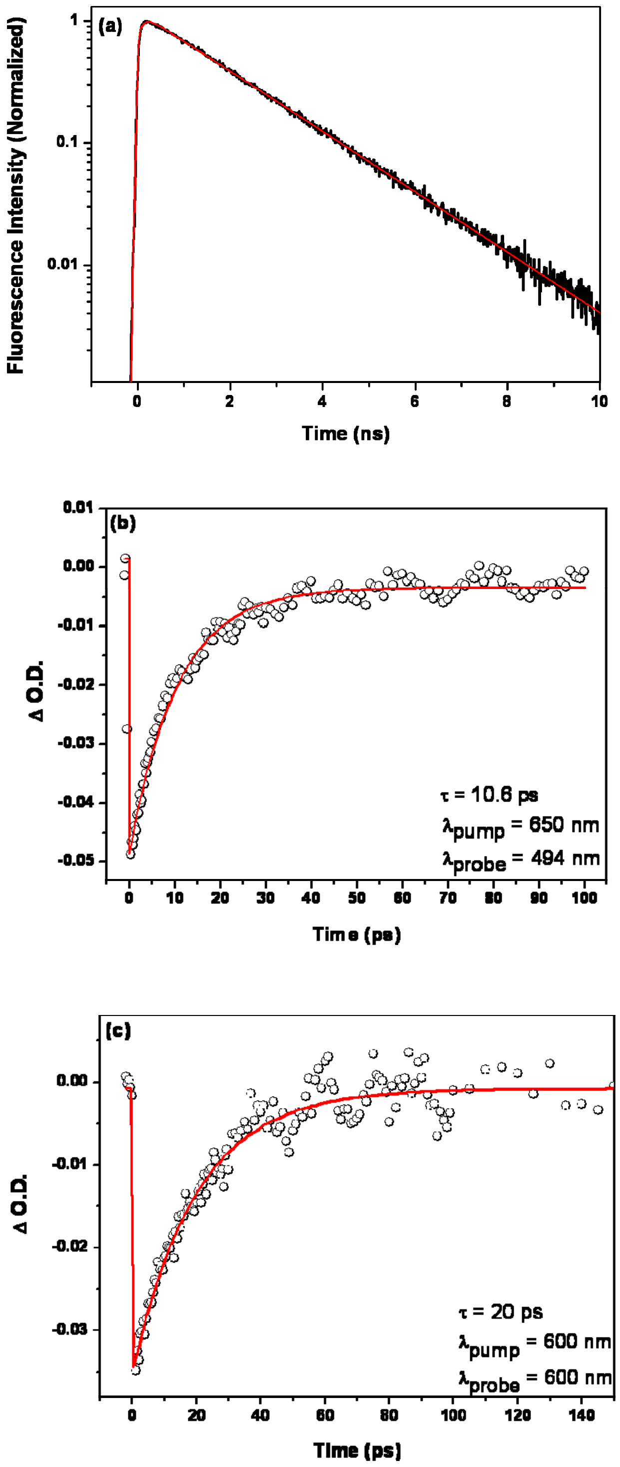

Fig. S3 Singlet excited-state decay profiles of (a) **NCP** (b) **NFP**, and (c) **N_2FP** in CH_2Cl_2. (a) The wavelength of pump excitation was 420 nm, and the wavelength of probe was 740 nm. (b) The wavelength of pump excitation was 650 nm, and the probe of bleaching was 494 nm. (c) The wavelength of pump excitation was 600 nm, and the probe of bleaching was 600 nm. The single exponential function was used to fit the experimental data (solid line).

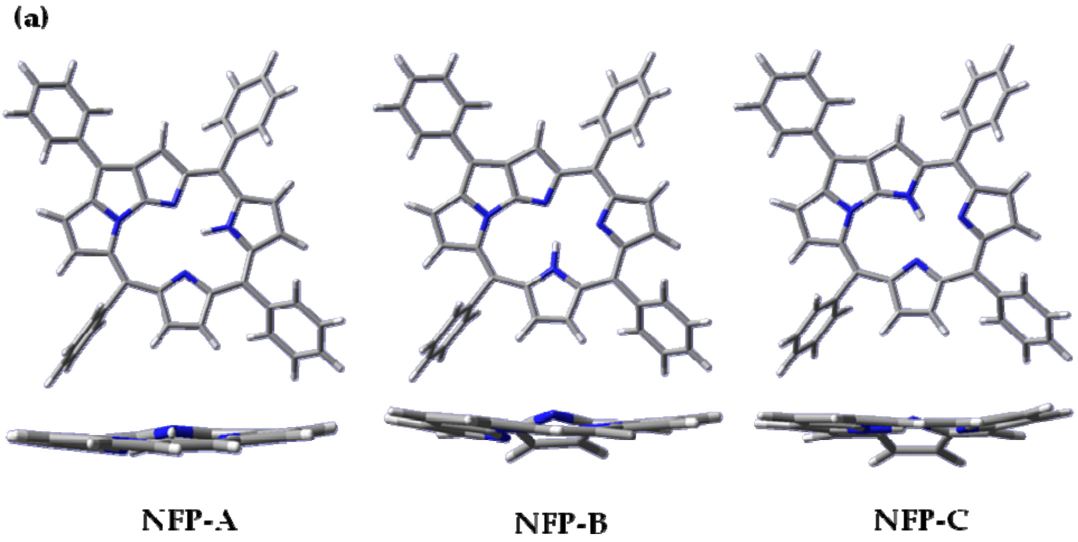

(b)

	Molecules		
	NFP-A	**NFP-B**	**NFP-C**
Energy (kcal/mol)	-1200107.58	-1200107.37	-1200102.81
Δ*E* (kcal/mol)	0	0.21	4.77

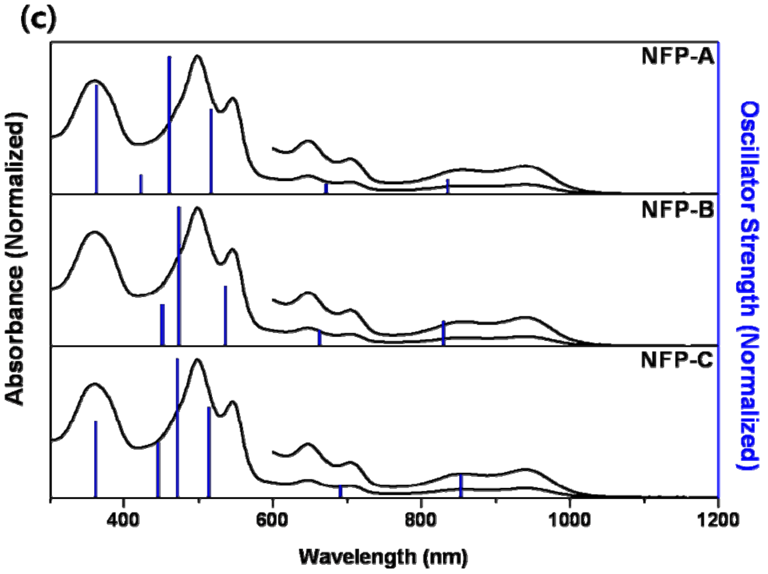

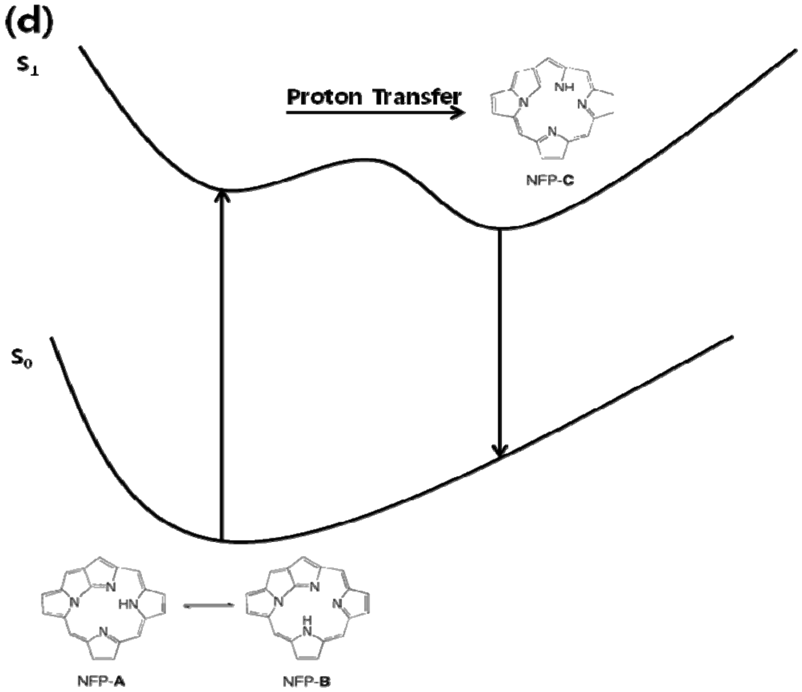

Fig. S4 Calculated (a) optimized molecular structures, (b) total energy, (c) oscillator strengths and (d) schematic representation of radiationless deactivation process of **NFP**-A, -B and -C.

NFP reveals strong hydrogen bonding of inner NH as analyzed by ^{1}H NMR spectra and as a consequence, structurally three types of tautomers can be considered (NFP-A, -B, and -C). In this regard, we have examined the differences of energies and structures in tautomers by theoretical calculations. As a result, we found that NFP-A and -B are more stable than NFP-C in the ground-state. However, one of possible tautomers (NFP-C) was found to be significantly deviated from planarity (0.2 Å) compared to NFP-A and -B having relatively planar geometries since the higher basicity of nitrogen in fused pyrrole rings by enhanced π-electron density as shown in AICD calculations is likely to weaken the hydrogen bonding ability (Fig. S1). Moreover, it was observed that structurally nonplanar tautomer (NFP-C) exhibits lower S_1 state energy than relatively planar tautomers (NFP-A, -B) having lower ground state energy by TDDFT calculation. Accordingly, we expect that NFP-C with out-of-plane distortion might provide very fast decay routes through photoinduced tautomerization. In summary, it is noteworthy that NH tautomerization processes play a major role in nonradiative decay processes, resulting in ultrafast decay of photoexcited **NFP**.

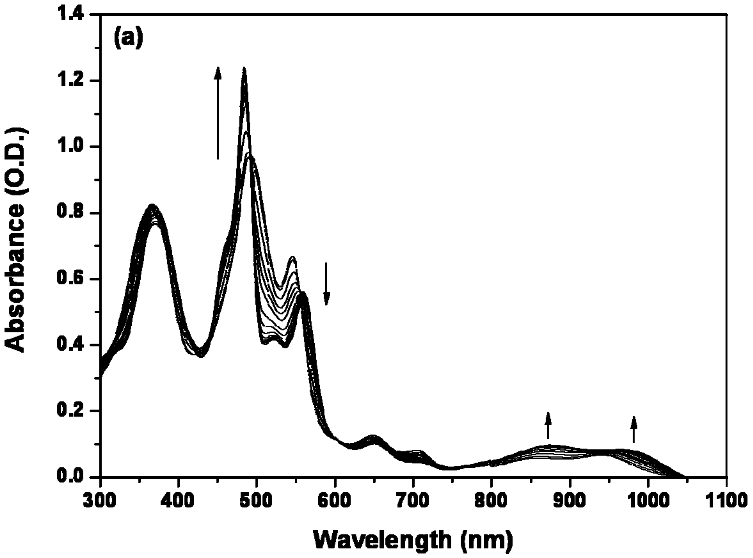

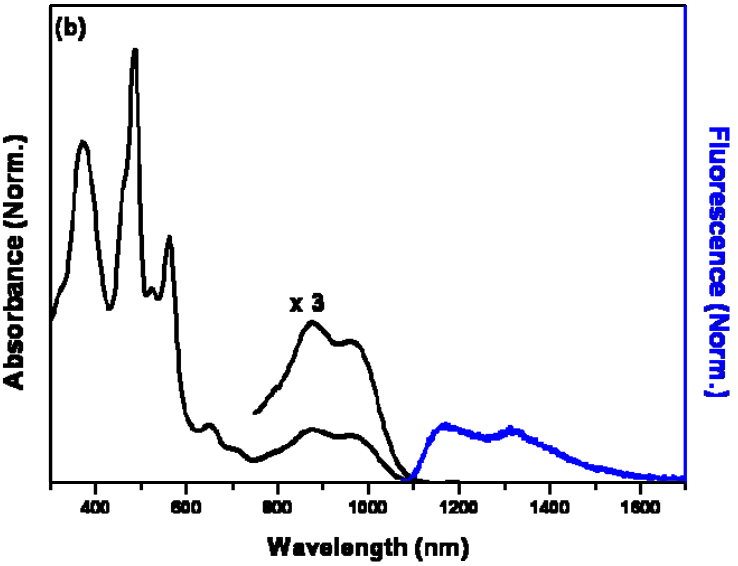

Fig. S5 UV-visible spectral changes during protonation of **NFP** by addition of TFA in CH_2Cl_2. (a) [TFA] from 0 to 1.4×10^{-1} M. (b) Fluorescence spectra of protonated species in **NFP**.

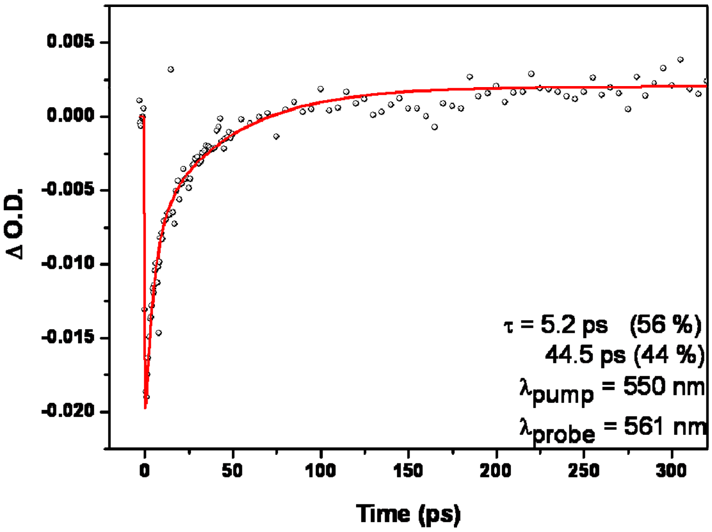

Fig. S6 Singlet excited-state decay profiles of protonated species in **NFP**. The pump excitation was at 550nm and the probe of bleaching was at 561nm.

References

(S1) Sheik-Bahae, M.; Said, A. A.; Wei, T. -H.; Hagan, D. G.; Van Stryland, E. W. *IEEE J. Quant. Electr.* **1990**, *26*, 760.

(S2) Kim, O. K.; Lee, K. S.; Woo, H. Y.; Kim, K. S.; He, G. S.; Swiatkiewicz, J.; Prasad, P. N. *Chem. Mater.* **2000**, *12*, 284.

(S3) Gaussian 03, Revision C.02, Frisch, M. J.; Trucks, G. W.; Schlegel, H. B.; Scuseria, G. E.; Robb, M. A.; Cheeseman, J. R.; Montgomery, Jr., J. A.; Vreven, T.; Kudin, K. N.; Burant, J. C.; Millam, J. M.; Iyengar, S. S.; Tomasi, J.; Barone, V.; Mennucci, B.; Cossi, M.; Scalmani, G.; Rega, N.; Petersson, G. A.; Nakatsuji, H.; Hada, M.; Ehara, M.; Toyota, K.; Fukuda, R.; Hasegawa, J.; Ishida, M.; Nakajima, T.; Honda, Y.; Kitao, O.; Nakai, H.; Klene, M.; Li, X.; Knox, J. E.; Hratchian, H. P.; Cross, J. B.; Bakken, V.; Adamo, C.; Jaramillo, J.; Gomperts, R.; Stratmann, R. E.; Yazyev, O.; Austin, A. J.; Cammi, R.; Pomelli, C.; Ochterski, J. W.; Ayala, P. Y.; Morokuma, K.; Voth, G. A.; Salvador, P.; Dannenberg, J. J.; Zakrzewski, V. G.; Dapprich, S.; Daniels, A. D.; Strain, M. C.; Farkas, O.; Malick, D. K.; Rabuck, A. D.; Raghavachari, K.; Foresman, J. B.; Ortiz, J. V.; Cui, Q.; Baboul, A. G.; Clifford, S.; Cioslowski, J.; Stefanov, B. B.; Liu, G.; Liashenko, A.; Piskorz, P.; Komaromi, I.; Martin, R. L.; Fox, D. J.; Keith, T.; Al-Laham, M. A.; Peng, C. Y.; Nanayakkara, A.; Challacombe, M.; Gill, P. M. W.; Johnson, B.; Chen, W.; Wong, M. W.; Gonzalez, C.; and Pople, J. A.; Gaussian, Inc., Wallingford CT, 2004.

(S4) Becke, A. D. *J. Chem. Phys.* **1992**, *98*, 1372.

(S5) Lee. C.; Yang, W.; Parr, R. G. *Phys. Rev. B.* **1988**, *37*, 785.

(S6) Keith, T. A.; Bader, R. F. W., *Chem. Phys. Lett.* **1992,** *194*, 1-8.

(S7) Keith, T. A.; Bader, R. F. W., *Chem. Phys. Lett.* **1993,** *210*, 223-231.

(S8) Cheeseman, J. R.; Trucks, G. W.; Keith, T. A.; Frisch, M. J., *J. Chem. Phys.* **1996,** *104*, 5497-5509.

(S9) Gaussview 4.1.2`; Gaussian, Inc.: Wallingford, CT, 2006.